

Size Effects and Charge-Density-Wave Pinning in NbSe₃

J. McCarten, M. Maher, T. L. Adelman, and R. E. Thorne

Laboratory of Atomic and Solid State Physics, Cornell University, Ithaca, New York 14853

(Received 19 September 1989)

We report measurements of the impurity-concentration and crystal-size dependences of the threshold field E_T for charge-density-wave (CDW) depinning in NbSe₃. These measurements establish that CDW's in Ta-doped NbSe₃ are weakly pinned. Size dependence of E_T occurs when the transverse crystal dimensions become comparable to the transverse CDW phase-phase correlation length, resulting in a crossover from 3D to 2D weak pinning. A divergence of the $T=4.2$ -K Ohmic resistance with decreasing sample thickness is attributed to diffuse scattering by crystal surfaces.

PACS numbers: 72.15.Nj

In quasi-one-dimensional metals such as NbSe₃, interaction between charge-density waves (CDW's) and impurities results in a variety of unusual transport effects.¹ Above a threshold electric field E_T , the CDW depins from the impurities and slides through the crystal, resulting in nonlinear dc conduction at fields of millivolts per centimeter.^{2,3} Coherent current oscillations observed in response to dc fields³ and mode-locking phenomena observed in response to combined ac and dc fields⁴ establish that this interaction is periodic in displacements of the CDW by integral numbers of CDW wavelengths λ (corresponding to CDW phase differences of $2n\pi$). Glassy behavior observed at low frequencies and at fields below threshold indicates that a randomly pinned CDW has many metastable configurations.

According to Fukuyama, Lee, and Rice (FLR),⁵ competition between the impurity energy gain associated with optimizing the CDW phase at each impurity site and the elastic energy cost associated with the required phase deformations between impurities determines the nature of the pinned state. In strong pinning the impurity energy dominates, and the CDW phase is pinned at each impurity; the CDW phase-phase correlation length L is then equal to the average impurity spacing. In weak pinning the elastic energy dominates, and the CDW phase is pinned on lengths L much greater than the average impurity spacing by fluctuations in the impurity potential. Qualitatively different behavior is predicted in these two regimes. In strong pinning $E_T \propto n_i$, while in weak pinning $E_T \propto n_i^2$, where n_i is the impurity concentration.

Early measurements by Brill *et al.*⁶ of the E_T - n_i relation in Ta- and Ti-doped NbSe₃ indicated that Ta, which is isoelectronic with Nb, acts as a weak pinning center while Ti, a charged impurity, acts as a strong pinning center. Subsequent measurements on Ta-doped NbSe₃ by Underweiser *et al.*⁷ indicated that $E_T \propto n_i$. Recently, the threshold field has been shown to increase with decreasing crystal cross-sectional area A (Ref. 8) and increasing surface-to-volume ratio.⁹ This increase has been attributed to CDW pinning by defects at crystal surfaces.⁹

Here we report measurements of both the impurity-concentration and the size dependences of the threshold field in NbSe₃. These measurements establish that CDW's in Ta-doped NbSe₃ are weakly pinned, and allow direct evaluation of important characteristic lengths. Size dependence of the threshold field occurs when the transverse crystal dimensions become comparable to the transverse CDW phase-phase correlation length, resulting in a crossover from 3D to 2D weak pinning.

NbSe₃ single crystals containing nominal Ta concentrations n_i between 0.01 and 0.3 at.% were prepared from the elements by vapor transport growth. The crystals grow as long ribbons consisting of stacked sheets of varying widths and thicknesses. The ribbon length, width, and thickness correspond to the crystallographic b , c , and a axes, respectively, with CDW motion occurring along the b axis. Crystal lengths can be several centimeters, widths vary from a fraction of a micron to a few hundred microns, and thicknesses are typically 5–10 times smaller than the width. Electrical measurements were made using a standard four-probe configuration. The length between voltage contacts and the extremal width w were measured using an optical microscope. The average thickness t (typically half the extremal thickness) was calculated from these dimensions and the measured room-temperature resistance, assuming $\sigma_z = 5.4 \times 10^3 \Omega^{-1} \text{cm}^{-1}$ (Ref. 10). Threshold-field measurements were made at 77 K, where the CDW order parameter and charge modulation amplitude are near their $T=0$ values. The residual resistivity ratio $r_R = R(300 \text{ K})/R(4.2 \text{ K})$ was used to characterize crystal purity.¹¹ For crystals with large cross-sectional areas, we find that r_R^{-1} is approximately proportional to the Ta impurity concentration estimated using emission spectroscopy, with $n_i r_R \approx 2 \times 10^{20} \text{cm}^{-3}$.

Following Ref. 9, Fig. 1 shows the dc threshold field E_T versus the circumference-to cross-sectional area ratio C/A (i.e., the surface-to-volume ratio) for 103 NbSe₃ crystals from four growths having different tantalum concentrations.¹² Crystal cross sections A vary by 4 orders of magnitude, from ~ 0.1 to $\sim 1000 \mu\text{m}^2$. For crystals with small C/A values, E_T is independent of sample

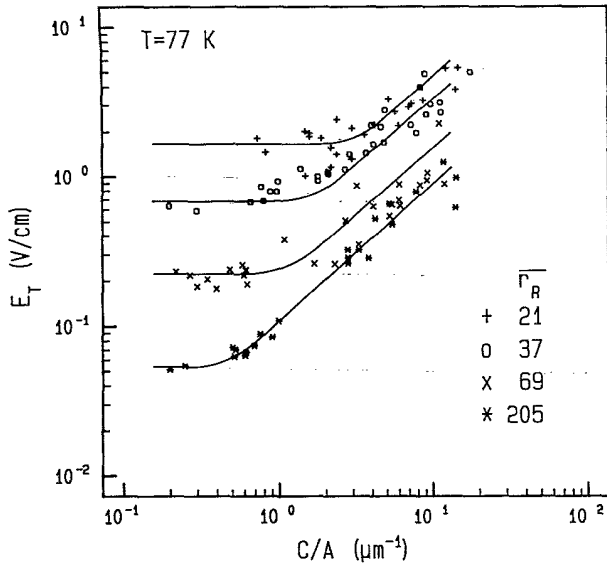


FIG. 1. Threshold electric field E_T at $T=77$ K vs the crystal circumference to cross-sectional area ratio C/A , for NbSe_3 crystals from four growths with different Ta concentrations. The r_R values represent averages for crystals with large cross sections. The solid lines are guides for the eye.

size. For large C/A , E_T varies approximately linearly with C/A . As the tantalum concentration (r_R^{-1}) increases, the crossover from the bulk to size-dependent regimes occurs for larger and larger C/A . NbSe_3 crystals used in previous transport studies have typically had $r_R \approx 100$ and cross-sectional areas between 10 and 100 μm^2 . The corresponding C/A values of between 0.5 and 2 μm^{-1} fall in the transition region between the bulk and size-dependent regimes.

Figure 2 shows E_T vs r_R^{-1} , proportional to the impurity concentration n_i , for 53 crystals in the bulk (small C/A) regime. The large scatter typical of such plots, as seen in Ref. 7, is eliminated by exclusion of crystals from the size-dependent regime. A least-squares fit yields

$$E_T(\text{V/cm}) = [(1.0 \pm 0.1) \times 10^3] r_R^{-b}, \quad b = 1.9 \pm 0.1. \quad (1)$$

The agreement with FLR's square-law prediction is excellent, providing strong evidence that CDW's in Ta-doped NbSe_3 are weakly pinned. Thresholds for the purest samples with r_R 's near 200 (indicated by circles in Fig. 2) fall slightly above the $E_T \propto r_R^{-2}$ line. Since further reducing the Ta concentration does not increase r_R , we attribute this deviation to pinning contributions by defects other than Ta atoms.

What is the origin of the size dependence of the threshold fit? One possibility is that the CDW is pinned by imperfections at crystal surfaces.⁹ Surface pinning should dominate over bulk impurity pinning in crystals with sufficiently large surface-to-volume ratios, and the threshold field should vary as $E_T = KC/A$, where K is a constant, independent of the bulk impurity concentra-

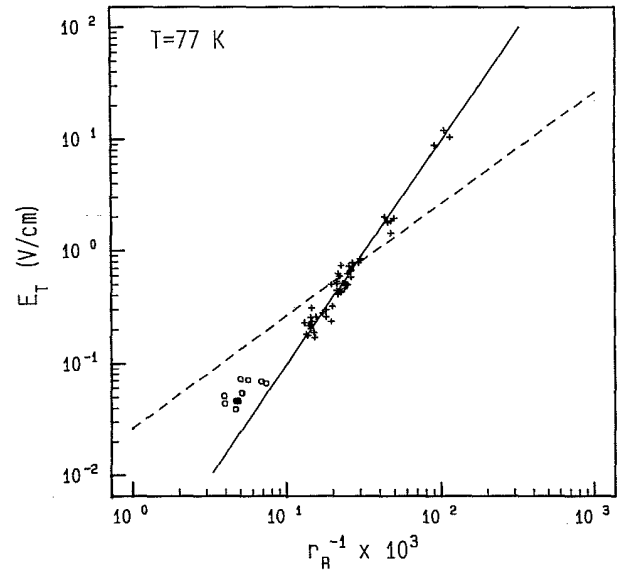


FIG. 2. Threshold electric field E_T at 77 K vs r_R^{-1} , proportional to the Ta impurity concentration, for NbSe_3 crystals in the size-independent regime. The solid and dashed lines correspond to $E_T \propto r_R^{-2}$ and $E_T \propto r_R^{-1}$, respectively. (O) crystals which were not intentionally doped (Ref. 12).

tion. However, while E_T in Fig. 1 is proportional to C/A , K appears to vary linearly with impurity concentration. Such behavior might result if the imperfections responsible for surface pinning were Ta atoms. This seems unlikely: Estimates using the experimental K values of the pinning strength of the surface Ta atoms are not significantly different from the bulk pinning strength. Furthermore, we find no evidence for increased pinning near crystal surfaces.¹³ Instead, the pinning appears to be homogeneous across the crystal cross section.

We believe that the size dependence of E_T is due to a crossover from three-dimensional to two- or one-dimensional weak pinning, which occurs when the transverse crystal dimensions impinge on the transverse CDW phase-phase correlation length. In 3D weak pinning the dc threshold field and longitudinal phase-phase correlation length L_z are given by^{5,14}

$$E_T^{(3D)} = \left[\frac{27}{\pi^3} \frac{(v\rho_1 A_0)^4}{e(\hbar v_F)^3} \right] n_i^2, \quad (2)$$

and

$$[L_z^{(3D)}]^2 = \left[\frac{\pi \hbar v_F}{3 e} \right] \frac{1}{E_T^{(3D)}}, \quad (3)$$

respectively, where v is the impurity potential, ρ_1 is the amplitude of the CDW charge modulation, A_0 is the cross-sectional area per chain, v_F is the Fermi velocity, and z is along the direction of CDW motion. The transverse phase-phase correlation lengths are related to L_z by $L_x = (\xi_x/\xi_z)L_z$ and $L_y = (\xi_y/\xi_z)L_z$. When the crystal thickness t becomes smaller than L_x , CDW phase defor-

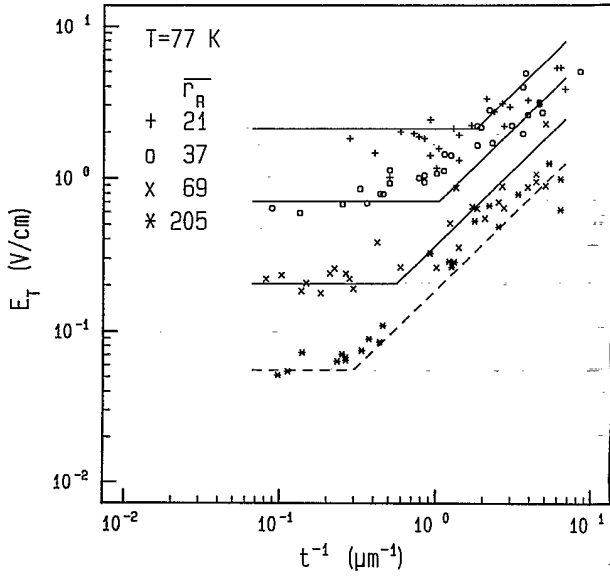


FIG. 3. Threshold electric field E_T at 77 K vs $1/t$, where t is the crystal thickness, for the NbSe₃ crystals of Fig. 1. The solid line represents the fits by Eqs. (1) and (5). The significance of the dashed line is explained in the text.

mations associated with pinning can no longer occur in this direction. For crystals with large aspect ratios w/t , the threshold field $E_T^{(2D)}$ is then given by

$$E_T^{(2D)} = \left[\frac{4}{\pi} \frac{(v\rho_1 A_0)^2}{e\hbar v_F} \frac{\xi_x}{\xi_z} \right] \frac{n_i}{t} \quad (4)$$

and varies linearly with impurity concentration and inversely with crystal thickness. Since $E_T^{(3D)} \approx E_T^{(2D)}$ when $t \approx 4L_x/3$, L_x can be estimated experimentally from the crystal thickness t_c below which E_T becomes size dependent.

Figure 3 shows E_T vs t^{-1} for the Ta-doped NbSe₃ crystals of Fig. 1. In the size-dependent regime, E_T does indeed vary approximately as t^{-1} . The solid lines represent the fit by Eq. (4) given by

$$E_T(\text{V/cm}) = (25 \pm 2) \frac{r_R^{-1}}{t(\mu\text{m})} \quad (5)$$

The strong resemblance to Fig. 1 results because most crystals have large w/t ratios so that $C/A = 2(t+w)/tw \approx 2/t$. No obvious correlation is observed between E_T and w . Scatter in the data results from factor-of-2 thickness variations across the width of typical crystals, and from aspect-ratio variations. Small crystals with $t \ll t_c$ often have widths $w < t_c$, so that the 1D weak-pinning limit $E_T \propto A^{-2/3}$ may apply.

In the present interpretation, the crystal thickness t_c at the crossover from bulk to size-dependent behavior must equal the 3D transverse phase-phase correlation length L_x deduced from the measured bulk threshold field. Equating Eq. (5) and a square-law fit to the data of Fig.

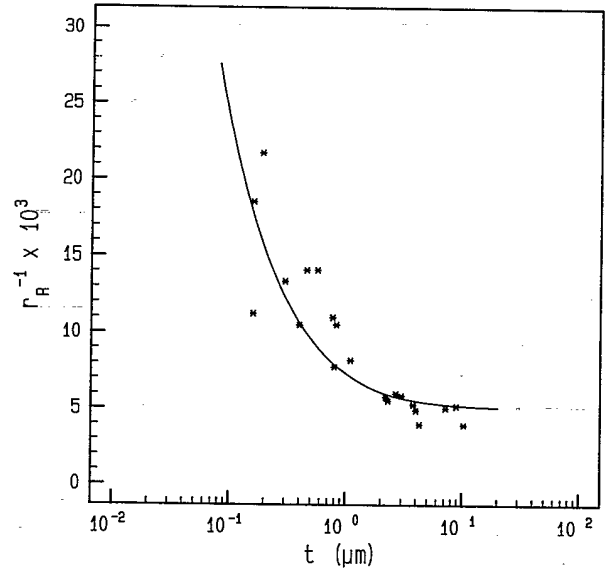


FIG. 4. r_R^{-1} vs crystal thickness t for NbSe₃ crystals containing ~ 100 -ppm Ta. The solid line is a fit by Fuch's theory of surface scattering, assuming 100% diffuse scattering and a transverse single-particle mean free path of $0.7 \mu\text{m}$.

2 yields

$$L_x(\mu\text{m}) \approx \frac{3}{4} t_c = 0.019 r_R \quad (6)$$

Using $v_F \approx 2.5 \times 10^7$ cm/s, $\xi_z/\xi_x \approx (\sigma_z/\sigma_x)^{1/2} = 7$,^{10,15,16} and the measured bulk threshold in Eq. (3) yields $L_x(\mu\text{m}) \approx 0.006 r_R$, consistent with Eq. (6) within the considerable uncertainties in our expressions.¹⁷ For the purest crystals, the fit provided by the dashed lines in Fig. 3 yields $3t_c/4r_R \approx 0.012 \mu\text{m}$. Even though defects other than Ta impurities contribute significantly to pinning in these crystals, the CDW's still appear to be weakly pinned.

The weak-pinning dimensionality-crossover model thus accounts both qualitatively and quantitatively for the impurity and size dependences of E_T in Ta-doped NbSe₃. Using this model, the $T=77$ -K longitudinal phase-phase correlation length in NbSe₃ crystals having $r_R \approx 100$ is estimated to be $17 \mu\text{m}$. The corresponding phase-coherent volume is enormous, involving $\sim 10^7$ parallel to Nb-Se chains and containing $\sim 10^8$ Ta impurities.

Crystals from a given growth show large scatter not only in their threshold fields, but also in their residual resistivity ratios r_R . Motivated by the results of Fig. 3, in Fig. 4 we plot r_R^{-1} versus crystal thickness for NbSe₃ crystals with Ta impurity concentration $n_i \approx 100$ ppm. The 4.2-K resistance diverges with decreasing crystal thickness for thicknesses below about $1 \mu\text{m}$. This behavior indicates significant carrier scattering from crystal surfaces; the sharpness of the divergence suggests that the scattering is mostly diffuse. The solid line in Fig. 4 is a fit by Fuch's theory of surface scattering,¹⁸ assuming

100% diffuse scattering. From this fit, we deduce a transverse mean free path for carriers on unnested portions of NbSe₃'s Fermi surface of $l_x \approx 0.7 \mu\text{m}$. Assuming that $l_z/l_x \approx \sigma_z/\sigma_x$, this implies a longitudinal mean free path at $T=4.2 \text{ K}$ of $35 \mu\text{m}$, consistent with that deduced from magnetotransport measurements.¹⁹

The present results have several implications for study of CDW's. First, weak pinning is shown to determine the CDW properties of the most widely studied material. Second, because of the large transverse correlation lengths in pure NbSe₃, CDW dynamics in three, two, and perhaps even one dimension can be investigated. Third, the phase-phase correlation length can now be directly determined from simple electrical measurements. A quantitative understanding of CDW pinning may soon be possible.

We wish to thank John Bardeen, J. Ross, F. Levy, and B. Horowitz for fruitful discussions, and B. Savord and D. DiCarlo for technical assistance. J.M. and R.E.T. gratefully acknowledge support provided by NSF and by the AT&T Foundation, the Alfred P. Sloan Foundation, and the NSF Materials Science Center at Cornell University, respectively.

¹For comprehensive reviews of CDW's, see *Electronic Properties of Quasi-One-Dimensional Materials*, edited by P. Monceau (Reidel, Dordrecht, 1985); G. Grüner, *Rev. Mod. Phys.* **60**, 1129 (1988).

²P. Monceau, N. P. Ong, A. M. Portis, A. Meerschaut, and J. Rouxel, *Phys. Rev. Lett.* **37**, 602 (1976).

³R. M. Fleming and C. C. Grimes, *Phys. Rev. Lett.* **42**, 1423 (1979).

⁴J. Richard, P. Monceau, and M. Renard, *Phys. Rev. B* **25**,

948 (1982); R. E. Thorne, W. G. Lyons, J. W. Lyding, J. R. Tucker, and John Bardeen, *Phys. Rev. B* **35**, 6360 (1987); **37**, 10055 (1988).

⁵H. Fukuyama and P. A. Lee, *Phys. Rev. B* **17**, 535 (1978); P. A. Lee and T. M. Rice, *Phys. Rev. B* **19**, 3970 (1979).

⁶J. W. Brill, N. P. Ong, J. C. Eckert, J. W. Savage, S. K. Khanna, and R. B. Somoano, *Phys. Rev. B* **23**, 1517 (1981).

⁷M. Underweiser, M. Maki, B. Alavi, and G. Grüner, *Solid State Commun.* **64**, 181 (1987).

⁸D. V. Bořodin, F. Ya. Nad', S. Savitskaja, and S. V. Zaitsev-Zotov, *Physica (Amsterdam)* **143B**, 73 (1986).

⁹P. J. Yetman and J. C. Gill, *Solid State Commun.* **62**, 201 (1987).

¹⁰T. J. Adelman, J. McCarten, M. Maher, and R. E. Thorne (to be published); J. Richard (private communication).

¹¹Ohmic conduction in NbSe₃ at low temperatures is by carriers on unnested portions of the Fermi surface.

¹²The purest of the four NbSe₃ growths was not intentionally doped. The ~ 100 -ppm Ta-doping level results from Ta present as impurities in the Nb source material.

¹³J. McCarten, T. L. Adelman, M. Maher, and R. E. Thorne (to be published).

¹⁴John Bardeen, *Z. Phys. B* **67**, 427 (1987).

¹⁵B. Horowitz, H. Gutfreund, and M. Weger, *Phys. Rev. B* **12**, 3174 (1975).

¹⁶Comparable values of ξ_z/ξ_x are obtained using band-structure calculations [S. Barisic in Ref. 1, p. 1, and R. Hoffmann, S. Shaik, J. C. Scott, M.-H. Whangbo, and M. J. Foshee, *J. Solid State Chem.* **34**, 263 (1980)] and using electrical conductivity measurements (Ref. 10).

¹⁷Equations (2)–(4) do not account for the effects of thermal fluctuations or partial Fermi-surface nesting, and assume that the CDW depins rigidly (i.e., that it loses its entire pinning energy when displaced by E_T through one-quarter wavelength).

¹⁸K. Fuchs, *Proc. Cambridge Philos. Soc.* **34**, 100 (1938).

¹⁹N. P. Ong and J. W. Brill, *Phys. Rev. B* **18**, 5265 (1978); N. P. Ong, *ibid.* **18**, 5272 (1978).